

# APATITE FISSION-TRACK AGES FOR THE VALDEZ GROUP AND THE PASSAGE CANAL AND BILLINGS PLUTONS, FROM THE PASSAGE CANAL AREA OF PRINCE WILLIAM SOUND, ALASKA

Robert J. Gillis<sup>1</sup> and Paul B. O'Sullivan<sup>2</sup>

Raw Data File 2024-30



Billings pluton freshly exposed at the toe of the retreating Billings Glacier, Prince William Sound, Alaska

This report has not been reviewed for technical content or for conformity to the editorial standards of DGGs.

2024  
STATE OF ALASKA  
DEPARTMENT OF NATURAL RESOURCES  
DIVISION OF GEOLOGICAL & GEOPHYSICAL SURVEYS



## **STATE OF ALASKA**

Mike Dunleavy, Governor

## **DEPARTMENT OF NATURAL RESOURCES**

John Boyle, Commissioner

## **DIVISION OF GEOLOGICAL & GEOPHYSICAL SURVEYS**

Melanie Werdon, State Geologist & Director

Publications produced by the Division of Geological & Geophysical Surveys are available to download from the DGGs website ([dgg.alaska.gov](https://dgg.alaska.gov)). Publications on hard-copy or digital media can be examined or purchased in the Fairbanks office:

### **Alaska Division of Geological & Geophysical Surveys (DGGs)**

3354 College Road | Fairbanks, Alaska 99709-3707

Phone: 907.451.5010 | Fax 907.451.5050

[dggspubs@alaska.gov](mailto:dggspubs@alaska.gov) | [dgg.alaska.gov](https://dgg.alaska.gov)

### **DGGs publications are also available at:**

Alaska State Library, Historical  
Collections & Talking Book Center  
395 Whittier Street  
Juneau, Alaska 99801

Alaska Resource Library and  
Information Services (ARLIS)  
3150 C Street, Suite 100  
Anchorage, Alaska 99503

### **Suggested citation:**

Gillis, R.J., and O'Sullivan, P.B., 2024, Apatite fission-track ages for the Valdez Goup and the Passage Canal and Billings plutons, from the Passage Canal area of Prince William Sound, Alaska: Alaska Division of Geological & Geophysical Surveys Raw Data File 2024-30, 8 p. <https://doi.org/10.14509/31428>



# **APATITE FISSION-TRACK AGES FOR THE VALDEZ GROUP AND THE PASSAGE CANAL AND BILLINGS PLUTONS, FROM THE PASSAGE CANAL AREA OF PRINCE WILLIAM SOUND, ALASKA**

Robert J. Gillis<sup>1</sup> and Paul B. O'Sullivan<sup>2</sup>

## **INTRODUCTION**

The following apatite fission-track (AFT) results supplement geologic mapping of the Passage Canal area near Whittier, Alaska (Bull and others, 2024) to constrain upper crustal cooling of major mapped bedrock units. These include Cretaceous Valdez Group marine strata and the Passage Canal and Billings plutons. Data associated with this report can be downloaded from <https://doi.org/10.14509/31428>.

## **LIST OF DELIVERABLES**

- Methods report
- Summary data spreadsheet and accompanying data dictionary
- Analytical lab data and accompanying data dictionary provided by GeoSep Services

## **METHODS**

### **Sample Collection**

We selected approximately 10–15 kg of the freshest, most unaltered and unweathered rock available at each of three sampled locations. Sample 12BG300A was a medium- to fine-grained sandstone metamorphosed to greenschist facies. Samples 12BG303A and 12BG308A were phaneritic intrusive rocks with unaltered mafic mineral phases, visible striae on crystal faces, and appeared to be free of chloritic alteration or oxidation. Sample locations were recorded using modern, hand-held GPS units set to UTM Zone 6 (NAD27) coordinates with typical horizontal precision of 9 to 21 feet. Locations presented herein were converted to NAD27 geographic coordinates.

### **Sample Preparation**

Each sample was crushed using a jaw crusher to <5 mm, and the crushate was sieved using 300-micron nylon mesh. The <300-micron fraction was washed with tap water and dried at room temperature in air, and zircon was isolated using standard gravimetric and magnetic mineral separation techniques. Apatite grains were mounted in epoxide resin and polished to a smooth finish using 0.3-micron alumina slurry. Apatite grain mounts were stirred vigorously in reagent-grade 5.5 molar nitric acid for 20 seconds at 21°C and rinsed with distilled water to remove any common lead contamination.

Apatite fission tracks were revealed by embedding the apatite grains in fluorinated ethylene propylene Teflon, polishing the grains to expose internal surfaces, and etching the fission tracks in a eutectic melt of NaOH-KOH at  $\sim 230^\circ\text{C}$  for 24–72 hours. Fission tracks were viewed and counted or measured at 1562.5x using a Zeiss Axioplan microscope with dry magnification using unpolarized, transmitted light with or without reflected light. All AFT age and length grains were selected to sample the greatest range of observable characteristics (size, degree of roundness, color, etch figure size, etc.).

### General ICP-MS Data Modeling

Steps for calculating the background intensity and its precision for an isotope at a spot were as follows:

1. The final background scan (background scan indicated by  $B_{scan}$ ) was determined programmatically as the first scan for which selected isotopic intensities were less than a preset number of subsequent scans; number of subsequent scans preset to 8; a spot analysis that did not exhibit common minima for the selected isotopes was deemed a failure; failure was usually due to loss of the grain after being dislodged by the laser or the grain was inaccessible to the laser within the sample cell during the LA-ICP-MS session. The first signal scan followed a preset number of scans (preset to 3) after the final background scan.
2. A line was fitted to  $B_{scan}$  values for each individual isotope by chi-squared minimization, outliers identified, and a line again fitted to  $B_{scan}$  values excluding the outliers.
3. For a fitted line exhibiting a negative slope (corresponding to decreasing  $B_{scan}$  values through time), the value of the fitted line at the first signal scan was calculated and assigned as the spot background intensity  $B_{spot}$ . For a fitted line exhibiting a zero or positive slope, the mean of  $B_{scan}$  values excluding the outliers was assigned as  $B_{spot}$ .

Background values for each isotope were smoothed session-wide using a running-median method as follows:

1. For structured background data, such as  $^{29}\text{Si}$ , which is highly influenced by atmospheric contamination from sample load to sample load, background data were smoothed using a running-median method characterized by a small window. Unstructured background data, such as  $^{206}\text{Pb}$ , were smoothed using a running-median method characterized by a large window.
2. For each window position, the regression line through included  $B_{spot}$  values gives a fitted  $B_{spot\_window}$  value at the spot;  $\sigma_{B_{spot\_window}}$  was evaluated as the absolute standard deviation of  $B_{spot}$  values within the window about the current fitted line for the window.
3. The number of  $B_{spot\_window}$  and  $\sigma_{B_{spot\_window}}$  values for the spot of interest equaled the number of scans defining the width of the window.
4. The session-wide, smoothed background intensity  $B_{spot\_smooth}$  for the isotope and spot of interest was taken as the median of the  $B_{spot\_window}$  values at each position of the running-median window.

5. The session-wide, smoothed absolute standard deviation of the background intensity  $\sigma_{B_{spot\_smooth}}$  for the isotope and spot of interest was taken as the median of the  $\sigma_{B_{spot\_window}}$  values at each position of the running-median window.

Steps for calculating background error at a spot were as follows:

1. For  $B_{spot} \leq B_{spot\_smooth} + 2\sigma_{B_{spot\_smooth}}$ ,  $\sigma_{B_{spot\_smooth}}$  was left unchanged.
2. For  $B_{spot} > B_{spot\_smooth} + 2\sigma_{B_{spot\_smooth}}$ ,  $\sigma_{B_{spot\_smooth}}$  was increased by  $0.5*(B_{spot} - B_{spot\_smooth})$ .

Raw signal intensities and their precisions were calculated as follows:

1. Individual scan raw signal intensities, (indicated by  $SB_{scan}$ ) were smoothed using a running-median method.
2. Scan background-corrected signal intensity  $S_{scan}$  was set equal to  $SB_{scan} - B_{spot\_smooth}$ .
3. All  $S_{scan}$  values for a spot were migrated in time, taking into account the acquisition times and mass differences between successively analyzed isotopes.

In the remainder of this paper, scan refers to an integer multiple of the time required to complete a single data collection scan and each  $S_{scan}$  value for a given scan represents a migrated value at fixed time.

Steps for calculating smoothed signal error at each signal scan at a spot were as follows:

1. The standard deviation of the non-outlier  $SB_{scan}$  values about their respective smoothed values was taken as the absolute signal intensity error  $\sigma_{S_{scan}}$  for each data scan, the value assumed constant for all scans at a spot.
2. The error for a single isotope at a single scan, the absolute  $\sigma_{scan\_isotope}$  was set equal to  $(\sigma_{S_{scan}}^2 + \sigma_{B_{spot\_smooth}}^2)^{0.5}$ .
3. The error of the sum of  $N$   $S_{scan}$  values for a particular isotope was taken as the product of  $N^{1/2} \sigma_{scan\_isotope}$ .

Sample  $^{238}\text{U}$  values were monitored for detection efficiency variations. In a session where  $^{235}\text{U}$  and  $^{238}\text{U}$  raw signals were directly measured, the  $^{238}\text{U}/^{235}\text{U}$  ratio was determined for each data scan at each spot. A regression of  $^{238}\text{U}$  signal (abscissa) versus  $^{238}\text{U}/^{235}\text{U}$  ratio (ordinate) was performed for all scans for which  $^{238}\text{U}$  exceeds some user-defined value. The results of this regression were presented to the user so that the user could: (A) use the resultant regression to correct  $^{238}\text{U}$  signals for detection efficiency bias, effectively rendering the  $^{238}\text{U}/^{235}\text{U}$  ratio independent of  $^{238}\text{U}$  signal; (B) adjust the user-defined  $^{238}\text{U}$  lower limit so that the data could be reprocessed and a new regression assessed; or (C) ignore the resultant regression and accept the  $^{238}\text{U}$  signal values in their uncorrected form. This process permits the user to identify evidence of and handle problems with pulse versus analog detection mode when  $^{238}\text{U}$  signal intensities are sufficiently high to overwhelm pulse detection mode.

### AFT and Data Analysis

ICP-MS data modeling and fission track ages were calculated using the scheme presented by Donelick and others (2005) using a modified zeta calibration approach after Hurford and Green (1983)

(see also Hasebe and others, 2004. The  $^{238}\text{U}/\text{primary cation}$  (primary cation  $^{43}\text{Ca}$  for apatite and  $^{91}\text{Zr}$  for zircon) for each data scan was calculated using the background-corrected signal values for the two isotopes as follows.

1. Each data scan was treated as a slice of ablated mineral where: (A) the thickness of the slice was determined by the  $S_{scan}$  value for primary cation multiplied by a calibration factor in terms of microns per primary cation, and (B) the depth of the slice was determined by the sum of the thicknesses of the overlying slices plus one half of the thickness of the current slice.
2. The  $S_{scan}$  value for  $^{238}\text{U}$  and the  $S_{scan}$  value for primary cation were used to calculate the  $^{238}\text{U}/\text{primary cation}$  ratio for each slice and a weighted sum for this ratio was calculated by weighting each slice according to: (A) slice thickness and (B) slice depth converted to the likelihood that fission tracks emanating from that depth could intersect the polished and etched mineral surface. Below  $l_0/2$  ( $l_0$  taken as the mean length of natural fission tracks in the zeta calibration standard), the likelihood of  $^{238}\text{U}$  contributing fission tracks to the etched apatite surface is effectively zero.
3. The absolute error of the weighted mean  $^{238}\text{U}/^{43}\text{Ca}$  ratio was calculated as follows (substitute  $^{91}\text{Zr}$  for  $^{43}\text{Ca}$  for zircon):

$$\sigma\left(\frac{^{238}\text{U}}{^{43}\text{Ca}}\right) = \left( N \left( \frac{\sigma_{\text{isotope-}^{43}\text{Ca}}}{\sum ^{43}\text{Ca}} \right)^2 + N \left( \frac{\sigma_{\text{isotope-}^{238}\text{U}}}{\sum ^{238}\text{U}} \right)^2 \right)^{1/2}$$

Where:

$\Sigma^{43}\text{Ca}$  = sum of  $S_{scan}$  values for  $^{43}\text{Ca}$  above a depth of  $l_0/2$

$\Sigma^{238}\text{U}$  = sum of  $S_{scan}$  values for  $^{238}\text{U}$  above a depth of  $l_0/2$

$N$  = number of scans above a depth of  $l_0/2$ .

Zeta age standard Durango (DR) was used as the apatite FT zeta age calibration standard. During each LA-ICP-MS session containing samples of unknown FT age, clusters of ~10 zeta spots were analyzed during the session for purposes of calibrating  $^{238}\text{U}/\text{primary cation}$ . Ratios of primary zeta (original zeta LA-ICP-MS session) to secondary zeta (current LA-ICP-MS session)  $^{238}\text{U}/^{43}\text{Ca}$  (apatite) or  $^{238}\text{U}/^{91}\text{Zr}$  (zircon) ratios were determined for each zeta calibration spot and smoothed using a load-specific running-median method. Only spots visited during the primary, original zeta LA-ICP-MS session were revisited during the secondary, current LA-ICP-MS session for this purpose. This method is analogous to using  $^{235}\text{U}$ -doped glass standards in the external detector method of fission track analysis (Donelick and others, 2005); in this study, specific DR grains from the primary standard LA-ICP-MS session serve as  $^{235}\text{U}$ -doped standards.

### AFT Inverse Thermal Modeling

Inverse thermal models of sample apatite ages and measured track lengths were produced using HeFTy v.1.9.3 software (Ketcham, 2005; copyright 2017, Richard A. Ketcham) and the annealing

model of Ketcham and others, 2007 (fig. 1). HeFTy model variables were set to the c-axis projection of Ketcham and others (2007) (5.0M), Cf irradiation, initial mean track length of 16.3  $\mu\text{m}$ , length reduction in standard of 0.893  $\mu\text{m}$ , and the Dpar kinetic parameter. Length data relied on the calibration mode KCH 2015 and Kuiper's statistic for calculating the goodness of fit. Age data relied on the LA-ICP-MS-G zeta mode with a lambda of 8.27266 and error of 0.10713.

Initial time-temperature constraints were based on the zircon U-Pb crystallization ages of the plutonic rocks analyzed from the same samples (Gillis and others, 2024) and a maximum depositional age of Valdez Group strata from the same sample (Gillis and others, 2024). The crystallization temperature for the plutonic rocks was set at a low 700°C because HeFTy becomes unstable at higher modeled temperatures (e.g., 800°C). A burial reheating constraint for the Valdez Group sample was based on its greenschist-facies metamorphic grade and is intentionally broad in time due to uncertainties about when maximum burial was reached. A second constraint allowed for potential partial reheating by nearby plutons. Each model was run until 50 good-fit paths were generated. For a discussion about the implications of the modeling results, see Bull and others (2024).

## RESULTS

### **Sample 12BG300A – Valdez Group: Maximum Depositional Age = 66.1±1.5 Ma**

Sample 12BG300A (Latitude/Longitude: 60.80260/-148.85042) is a fine-upper to medium-lower-grained, moderately sorted sandstone with subrounded to subangular grains. The sample is metamorphosed to greenschist facies and outcrops near minor medium-bedded slate with possible weak S-C fabric parallel to bedding.

It produced a pooled age of 18.7+5.5/-4.3 Ma with a measured mean track length (MTL) of 14.17±0.12  $\mu\text{m}$  and a Dpar value of 2.33 (fig. 1). An inverse thermal model of the data suggests cooling at a rate of approximately 13.5°C/m.y. from about 16.5 to 11.5 Ma.

### **Sample 12BG303A – Passage Canal Pluton: Crystallization Age = 38.7±0.9 Ma**

Sample 12BG303A (Latitude/Longitude: 60.86881/-148.49242) Granite composed of 34 percent granophyric potassium feldspar crystals 3 mm to 1 cm long with Carlsbad twinning and plagioclase inclusions. Quartz crystals 2 mm to 1 cm long constitute 34 percent of the sample with overgrowths on some crystals and tiny unidentified inclusions. Undulose extinction and embayed, cracked quartz crystals are common. The rock consists of 24 percent plagioclase crystals with sericite and lamellar twins, 2 to 4 mm long. Biotite crystals (3 percent) are variably altered to chlorite, and exhibit dark red-brown and light brown pleochroism; some show birds-eye extinction. The sample also contains trace muscovite and opaques (the latter often enclosed within altered biotite).

The sample produced a pooled age of 18.7+5.5/-4.3 Ma with a measured MTL of 13.92±0.15  $\mu\text{m}$  and a Dpar value of 2.16 (fig. 1). An inverse thermal model of the data suggests cooling at a rate of approximately 30°C/m.y. from about 18.4 to 16.8 Ma.

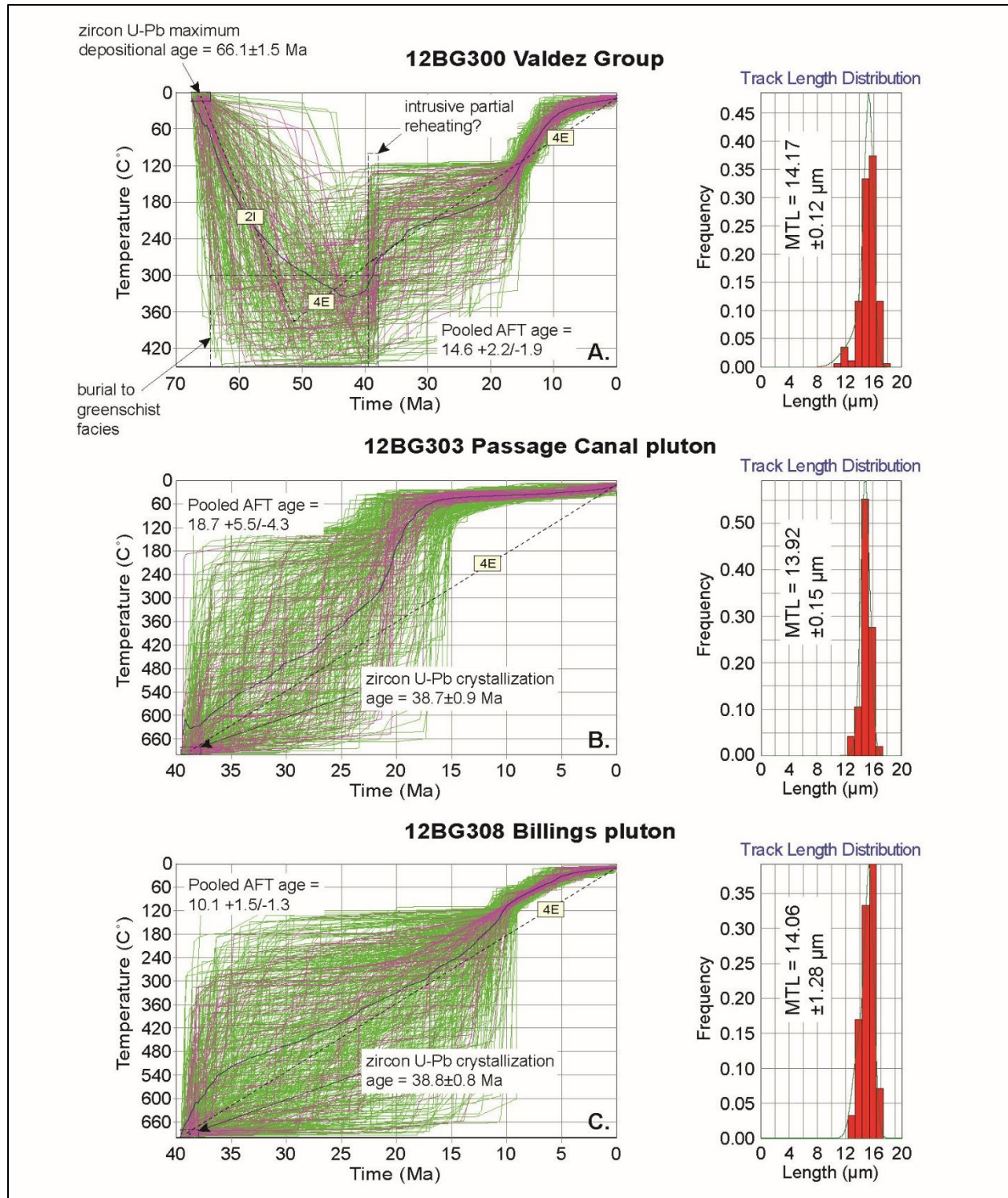


**Figure 1.** Inverse thermal model results and C-axis projected track length distributions for samples 12BG300 (A), 12BG303 (B), and 12BG308 (C).



### **Sample 12BG308A – Billings Pluton: Crystallization Age = $38.8 \pm 0.8$ Ma**

12BG308A (Latitude/Longitude: 60.85443/-148.59760) Granite consisting of 34 percent granophyric potassium feldspar crystals 3 mm to 1 cm long with Carlsbad twinning and plagioclase inclusions. Thirty-four percent quartz crystals 2 mm to 1 cm long with overgrowths on some crystals and tiny unidentified inclusions. Common undulose extinction and embayed, cracked crystals. Twenty-four percent plagioclase 2 to 4 mm long, commonly with sericite and lamellar twins. Three to 5 percent biotite, mostly altered to chlorite with dark red-brown and light brown pleochroism; some birds-eye extinction. Some muscovite and trace opaques (the latter often within altered biotite). Plagioclase and potassium feldspars exhibit possible perthitic textures.

This sample produced a pooled age of  $18.7 + 5.5 / - 4.3$  Ma with a measured MTL of  $14.51 \pm 0.44$   $\mu\text{m}$  and a Dpar value of 2.11 (fig. 1). An inverse thermal model of the data suggests cooling at a rate of approximately  $15^\circ\text{C}/\text{m.y.}$  from about 10 to 7 Ma.

### **ACKNOWLEDGEMENTS**

We thank Pathfinder Aviation and pilot Spanky Handley for exceptional work in difficult circumstances, and the people of Whittier for their kindness and generosity. We greatly appreciate the Chugach Alaska Native Corporation and the U.S. Forest Service for their helpfulness and access to their lands during this study.

These analyses were funded by the 2012 U.S. Geological Survey National Cooperative Geologic Mapping Program, award number G12AS00007. The views and conclusions contained in this document are those of the authors and should not be interpreted as representing the opinions or policies of the U.S. Geological Survey. Mention of trade names or commercial products does not constitute their endorsement by the U.S. Geological Survey.

### **REFERENCES**

- Bull, K.F., Stevens, D.S.P., Gillis, R.J., Wolken, G.J., and Balazs, M.S., 2024, Geology and geologic hazards of the Whittier area, Southcentral Alaska: Alaska Division of Geological & Geophysical Surveys Preliminary Interpretive Report Data File 2024-4, 18 p., 1 sheet.  
<https://doi.org/10.14509/31426>
- Donelick, R.A., O'Sullivan, P.B., Ketcham, R.A., 2005, Apatite fission-track analysis: Reviews in Mineralogy and Geochemistry, Mineralogical Society of America, v. 58, p. 49–94.
- Gillis, R.J., O'Sullivan, P.B., and Donelick, R.A., 2024, Zircon U-P ages of the Valdez Group, Passage Canal, and Billings plutons from the Passage Canal area of Prince William Sound, Alaska: Alaska Division of Geological & Geophysical Surveys Raw Data File 2024-29, 11p.  
<https://doi.org/10.14509/31427>
- Hasebe, Noriko, Barbarand, Jocelyn, Jarvis, Kym, Carter, Andrew, Hurford, A.J., 2004, Apatite fission-track chronometry using laser ablation ICP-MS: Chemical Geology, v. 207, p. 135–145.  
<https://doi.org/10.1016/j.chemgeo.2004.01.007>

- Hurford, A.J., and Green, P.F., 1983, The zeta age calibration of fission-track dating: *Isotope Geoscience*, v. 1, p. 285–317.
- Ketcham, R.A., 2005, Forward and inverse modeling of low-temperature thermochronometry data: *Reviews in Mineralogy and Geochemistry*, v. 58, no. 1, p.275–314.
- Ketcham, R.A., Carter, Andrew, Donelick, R.A., Barbarand, Jocelyn, and Hurford, A.J., 2007, Improved modeling of fission-track annealing in apatite: *American Mineralogist*, v. 92, no 5–6, p. 799–810.